

Monolithically integrated AlGaIn/GaN/AlN-based solar-blind ultraviolet and near-infrared detectors

D. Hofstetter, R. Theron, E. Baumann, F.R. Giorgetta, S. Golka, G. Strasser, F. Guillot and E. Monroy

D. Hofstetter, R. Theron, E. Baumann and F.R. Giorgetta (*Institute of Physics, University of Neuchatel, 1 A.-L. Breguet, Neuchatel CH-2000, Switzerland*)

E-mail: daniel.hofstetter@unine.ch

S. Golka and G. Strasser (*Technical University of Vienna, Vienna A-1040, Austria*)

F. Guillot and E. Monroy (*CEA Grenoble, INAC/SP2M/NPSC, 17 Rue des Martyrs, F-38054, France*)

Closely spaced, monolithically integrated photodetectors in two largely different wavelengths ranges are demonstrated. The device structure was grown by plasma-assisted molecular-beam epitaxy on an AlN-on-sapphire template, and it consists of a Si-doped AlGaIn thin film, and a nearly strain compensated 40 period AlN/GaN superlattice with 1.0 nm-thick GaN quantum wells and 2.0 nm-thick AlN barriers. The entire structure is covered with an AlGaIn cap. The superlattice constitutes the active region for the infrared detector, while the AlGaIn buffer layer serves as active area for the ultraviolet detector. The photoconductive ultraviolet detector has a long wavelength cutoff at 250 nm, whereas the photovoltaic near-infrared detector has a centre wavelength of 1.37 μm .

Multispectral cameras operating in entirely different wavelength ranges such as ultraviolet (UV), visible, or even the infrared (IR) are attracting increasing interest for applications in surveillance, failure analysis, and meteorology [1]. Up to now, such multispectral imaging systems have been fabricated by overlaying visible and UV pictures coming from two different image sensor arrays. Although this solution has the advantage of offering optimised performances for both wavelength ranges, it requires use of several bulky and rather expensive optical components. In addition, such a system is relatively sensitive for shocks or vibrations, and therefore not totally reliable for in-the-field applications. Systems being up to this challenge are therefore very expensive. A monolithic integration of two or even three operation wavelengths into a single camera chip could thus offer several advantages over existing solutions, notably in terms of price, robustness, and flexibility. Unfortunately, there are not many semiconductor materials which would allow a monolithic integration of all three wavelength ranges mentioned above. In addition, most semiconductors having sufficiently dissimilar bandgap energies suffer from large lattice mismatches, even within the same family [2]. For this reason, a different solution involving not only interband, but also intersubband transitions, must be pursued. One possible way which is presented in this Letter is the integration of a photoconductive UV interband detector based on an AlGaIn thin film [3] and a photovoltaic near-IR intersubband detector based on an AlN/GaN superlattice [4–6]. In a first demonstration, we show a UV/IR detector pair with only 350 μm separation between the UV and IR device. Both detectors exhibit spectrally narrow responsivity curves, which enlarges the UV-to-visible rejection ratio in the case of the UV device, and which improves the noise behaviour in the case of the IR detector.

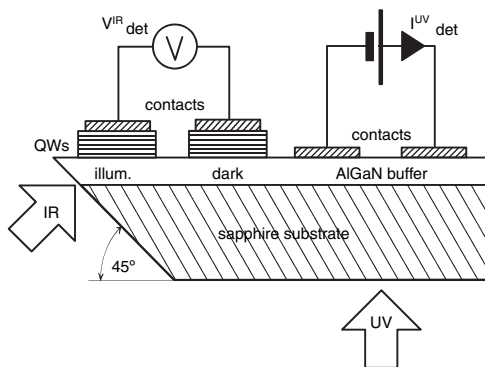


Fig. 1 Schematic cross-section through sample showing relative positions of UV and IR detector

QWs used as detection layer for IR, while AlGaIn buffer is detection layer for UV radiation

Fabrication of this prototype dual wavelength detector was based on a series of layers epitaxially grown by plasma-assisted molecular-beam epitaxy on a commercial AlN-on-sapphire template. First, a 250 nm-thick Si-doped ($[\text{Si}] \sim 5 \times 10^{19} \text{ cm}^{-3}$) $\text{Al}_{0.65}\text{Ga}_{0.35}\text{N}$ thin film was grown, followed by a regular 40 period superlattice with 1.0 nm-thick Si-doped GaN quantum wells ($[\text{Si}] \sim 1 \times 10^{19} \text{ cm}^{-3}$) and 2.0 nm-thick AlN barriers. The structure was then capped with a 5 nm-thick $\text{Al}_{0.65}\text{Ga}_{0.35}\text{N}$ cap layer. Using reactive ion etching, the wafer was then mesa-structured to a depth of roughly 150 nm. The UV detectors were fabricated in those areas where the superlattice had been etched down to the $\text{Al}_{0.65}\text{Ga}_{0.35}\text{N}$ buffer layer. They consist of two simple, rectangularly shaped $50 \times 100 \mu\text{m}^2$ large, alloyed ohmic metal contacts (Ti/Al/Ti/Au, 20/170/5/500 nm). On the other hand, the IR detectors are fabricated from rectangularly shaped Schottky contacts of $50 \times 100 \mu\text{m}^2$ size (Ti/Au, 10/500 nm) evaporated directly on the as-grown areas. Wire bonds were used to establish an electrical connection between the detector contacts and the larger ceramic contact pads on the chip holder. A schematic cross-section through the layer structure and the devices is shown in Fig. 1, while a typical microscope picture of the chip with the corresponding bonding wires is presented in Fig. 2. The relative positions of the relevant detector contacts are highlighted by encircling for both the UV and the IR detector. The separation between the UV and the IR device is 350 μm .

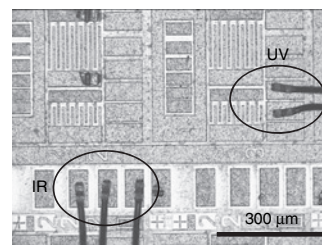


Fig. 2 Microscope photograph of sample showing bonded detectors and their separation on the chip

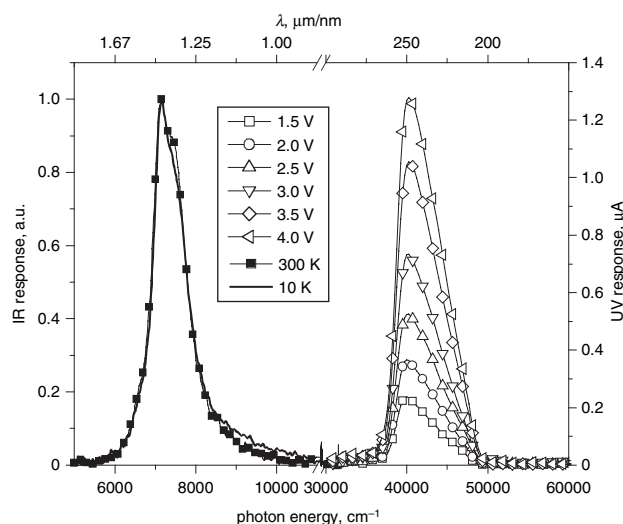


Fig. 3 Measured spectral responsivity curves for UV (1.5 to 4.0 V in steps of 0.5 V at 300 K) and IR detector (10 and 300 K)

For characterisation of the UV detector, we used a Fourier transform spectrometer equipped with an external deuterium lamp, and a CaF₂ beam splitter. The beam of the UV lamp was chopped at low frequency ($f = 6.66$ Hz), and focalised onto the detector from the substrate side; the resulting electrical signal was amplified in a lock-in amplifier and fed into the external detector port of the spectrometer. A Keithley sourcemeter provided the necessary bias voltage to operate the UV detector in photoconductive mode. Owing to the slow response time of the UV detector, the measurements were performed in step-scan modulation using a dwell time of the order of 500 ms. Measurements at six different bias voltages ranging from 1.5 to 4 V were recorded at room temperature. Characterisation of the IR detector was based on illumination of one of the two contacts of the device via a 45° polished facet using an internal white light source, and the CaF₂ beam splitter of the Fourier spectrometer. Acquisition of the photovoltaic signal was accomplished via an SR570 amplifier, and direct feeding of the amplified voltage into the external port of the spectrometer. Spectra were taken at various temperatures between 10 K and room temperature with the sample being mounted in a liquid He flow cryostat. Fig. 3 shows the optical characteristics of the two detectors. The spectra of the IR device recorded at temperatures of 10, 50, 100, 150, 200, 250, and 300 K show about 10% difference in responsivity; therefore, only the 10 and the 300 K spectrum are presented. The responsivity peak position is at 7280 cm^{-1} (910 meV, $1.37\text{ }\mu\text{m}$) with a full width at half maximum of 925 cm^{-1} (116 meV). The UV device was tested at room temperature only; it shows a pronounced signal increase with increasing bias voltage. The responsivity peaks at $40\,000\text{ cm}^{-1}$ (5 eV, 250 nm) and has a full width at half maximum of roughly $5\,000\text{ cm}^{-1}$ (0.67 eV). Its long wavelength cutoff at about 4.9 eV is determined by the bandgap energy of the AlGa_N active layer, while the short wavelength cutoff at 6.2 eV is due to strong band-to-band absorption in the underlying AlN growth template layer. Introduction of an additional AlGa_N layer with a higher Al content would result in a much sharper cutoff on the short wavelength side, and thus a considerably narrower responsivity peak. The voltage responsivity of the IR detector is roughly 10 V/W, while the best current responsivity of the UV device lies of the order of 10 mA/W.

In future measurements and based on experiments with more recently grown epitaxial material, we expect substantial improvements of these values.

Conclusion: We have demonstrated a monolithic integration of a solar-blind UV detector and a narrowband near-IR detector. The two devices function up to room temperature and are separated by only 350 μm . This demonstration is a first important step towards multispectral cameras containing in each pixel UV, near-visible, and IR sensitive imaging elements.

Acknowledgments: The authors wish to thank the European project NitWave (004170), and the Professorship Program and the NCCR ‘Quantum Photonics’, both sponsored by the Swiss National Science Foundation. AlN-on-sapphire templates were provided by DOWA Electronics Materials Inc.

References

- 1 See for instance http://www.ofil.co.il/Products/range_of_products.html
- 2 Strite, S.T., and Morkoc, H.: ‘Ga_N, Al_N, and In_N: a review’, *J. Vac. Sci. Technol. B*, 1992, **10**, (4), pp. 1237–1266
- 3 Monroy, E., Calle, F., Munoz, E., Ommes, E., Beaumont, B., and Gibart, P.: ‘Visible-blindness in photoconductive and photovoltaic AlGa_N ultraviolet detectors’, *J. Electron. Mater.*, 1998, **28**, (3), pp. 240–245
- 4 Hofstetter, D., Schad, S.-S., Wu, H., Schaff, W.J., and Eastman, L.F.: ‘Ga_N/Al_N-based quantum well infrared photodetector for $1.55\text{ }\mu\text{m}$ ’, *Appl. Phys. Lett.*, 2003, **83**, (3), pp. 572–574
- 5 Hofstetter, D., Baumann, E., Giorgetta, F.R., Graf, M., Maier, M., Guillot, F., Bellet-Amalric, E., and Monroy, E.: ‘High-quality Al_N/Ga_N-superlattice structures for the fabrication of narrow-band $1.4\text{ }\mu\text{m}$ photovoltaic intersubband detectors’, *Appl. Phys. Lett.*, 2006, **88**, (12), pp. 121112
- 6 Hofstetter, D., Baumann, E., Giorgetta, F.R., Guillot, F., Leconte, S., and Monroy, E.: ‘Optically non-linear effects in intersubband transitions of Ga_N/Al_N-based superlattices’, *Appl. Phys. Lett.*, 2007, **91**, (13), pp. 131115